PNAS RESEARCH ARTICLE | PHARMACOLOGY

Therapeutic antagonism of the neurokinin 1 receptor in endosomes provides sustained pain relief

Alan Hegron[a,b,c,1], Chloe J. Peach[a,b,c,1], Raquel Tonello[a,b,c,1], Philipp Seemann[d,1], Shavonne Teng[a,b,c], Rocco Latorre[a,b,c], Harald Huebner[d], Dorothee Weikert[d], Jeanette Rientjes[e], Nicholas A. Veldhuis[f], Daniel P. Poole[f], Dane D. Jensen[a,b,c,g], Alex R. B. Thomsen[a,b,c], Brian L. Schmidt[a,b,c,g], Wendy L. Imlach[h], Peter Gmeiner[d], and Nigel W. Bunnett[a,b,c,2]

Edited by Robert Lefkowitz, Howard Hughes Medical Institute, Durham, NC; received December 9, 2022; accepted April 4, 2023

The hypothesis that sustained G protein-coupled receptor (GPCR) signaling from endosomes mediates pain is based on studies with endocytosis inhibitors and lipid-conjugated or nanoparticle-encapsulated antagonists targeted to endosomes. GPCR antagonists that reverse sustained endosomal signaling and nociception are needed. However, the criteria for rational design of such compounds are ill-defined. Moreover, the role of natural GPCR variants, which exhibit aberrant signaling and endosomal trafficking, in maintaining pain is unknown. Herein, substance P (SP) was found to evoke clathrin-mediated assembly of endosomal signaling complexes comprising neurokinin 1 receptor (NK_1R), $G\alpha_{q/i}$, and βarrestin-2. Whereas the FDA-approved NK_1R antagonist aprepitant induced a transient disruption of endosomal signals, analogs of netupitant designed to penetrate membranes and persist in acidic endosomes through altered lipophilicity and pKa caused sustained inhibition of endosomal signals. When injected intrathecally to target spinal NK_1R+ve neurons in knockin mice expressing human NK_1R, aprepitant transiently inhibited nociceptive responses to intraplantar injection of capsaicin. Conversely, netupitant analogs had more potent, efficacious, and sustained antinociceptive effects. Mice expressing C-terminally truncated human NK_1R, corresponding to a natural variant with aberrant signaling and trafficking, displayed attenuated SP-evoked excitation of spinal neurons and blunted nociceptive responses to SP. Thus, sustained antagonism of the NK_1R in endosomes correlates with long-lasting antinociception, and domains within the C-terminus of the NK_1R are necessary for the full pronociceptive actions of SP. The results support the hypothesis that endosomal signaling of GPCRs mediates nociception and provides insight into strategies for antagonizing GPCRs in intracellular locations for the treatment of diverse diseases.

signaling | receptors | endocytosis | pain

G protein-coupled receptors (GPCRs) are seven transmembrane domain receptors for hormones and neurotransmitters. They control homeostatic and disease processes and are therapeutic targets for disease (1). Drug discovery has focused on targeting GPCRs at the cell surface. However, plasma membrane signaling of GPCRs is usually tightly regulated and may not exclusively mediate long-lasting pathology. After binding to extracellular ligands, GPCRs are phosphorylated by GPCR kinases (GRKs) and interact with βarrestins (βARRs), which uncouple GPCRs from G proteins and desensitize plasma membrane signaling (2, 3). βARRs also couple GPCRs to clathrin and adaptor protein-2, which leads to dynamin (Dnm)-mediated vesicle scission and mediates receptor endocytosis. Although endocytosis has been considered as a mechanism that terminates GPCR signaling, many GPCRs continue to signal after endocytosis, including most class B GPCRs that interact with βARRs with sustained kinetics and some class A GPCRs that exhibit transient interactions with βARRs (4–15). Within endosomes, GPCR, Gα, and/or βARR signaling complexes (signalosomes) generate second messengers and activate kinases in subcellular compartments. Endosomal signaling of GPCRs has been implicated in certain physiological and pathological processes, including hormonal control (4, 7) and pain transmission (9–11, 15–17). Thus, GPCRs in endosomes, rather than at the cell surface, might be the optimal therapeutic target (18).

Painful stimuli provoke the release of substance P (SP) from primary sensory neurons, which stimulates endocytosis of the neurokinin 1 receptor (NK_1R) in second-order spinal neurons and endothelial cells of postcapillary venules (9, 19). NK_1R signals in endosomes mediate sustained activation of spinal neurons and pain transmission (9, 17). The calcitonin-like receptor (15), protease-activated receptor 2 (11, 16), and ∂-opioid receptor (10) also signal from endosomes to control pain, which suggests a general role for endosomal GPCR signaling in pain. The hypothesis that endosomal GPCR signaling controls nociception derives from the use of endocytosis inhibitors, which suppress endosomal signaling

Significance

Sustained GPCR signaling from endosomes mediates pathologies, including pain. Optimal therapy requires development of antagonists that penetrate cells, are retained in endosomes, and disrupt endosomal signaling. To enhance membrane penetration and retention in acidified endosomes, analogs of the neurokinin 1 receptor (NK_1R) antagonist netupitant were synthesized with altered lipophilicity and acidity. Lipophilic and acidic analogs antagonized endosomal NK_1R signaling and provided potent, efficacious, and long-lasting pain relief in mice expressing human NK_1R. Mice expressing a truncated NK_1R, corresponding to a naturally occurring variant with aberrant signaling and trafficking, showed diminished nociceptive responses to substance P. The results identify criteria that will facilitate the design of antagonists of endosomal receptors and provide evidence for the contribution of endosomal signaling to disease.

Competing interest statement: N.W.B. is a founding scientist of Endosome Therapeutics Inc. Research in N.W.B.'s laboratory is funded, in part, by Takeda Pharmaceuticals International.

This article is a PNAS Direct Submission.

[1]A.H., C.J.P., R.T., and P.S. contributed equally to this work.

[2]To whom correspondence may be addressed. Email: nwb2@nyu.edu.

This article contains supporting information online at https://www.pnas.org/lookup/suppl/doi:10.1073/pnas.2220979120/-/DCSupplemental.

Published May 22, 2023.

and nociception (9, 11). Preferential blockade of endosomal GPCRs has been achieved by antagonist conjugation to a transmembrane lipid or encapsulation into nanoparticles, which deliver antagonists to endosomes and provide sustained antinociception (9–11, 15, 17, 20–22). Pharmacokinetic considerations may restrict the usefulness of lipidated and nanoparticle-encapsulated GPCR antagonists. The criteria for rational design of small-molecule GPCR antagonists that penetrate plasma and endosomal membranes, disrupt assembly of multiprotein signalosomes in acidic endosomes, and reverse sustained endosomal signaling and nociception are ill-defined. Whether expression of GPCR variants unable to signal from endosomes confers resistance to pain is unknown.

The current study sought to define the criteria for designing GPCR antagonists that disrupt endosomal signalosomes and provide effective pain relief. The NK_1R antagonists aprepitant (AP) and netupitant (NT), which are both FDA approved for treatment of chemotherapy-induced nausea and vomiting (23, 24), were compared with NT analogs with differing lipophilicity (LogP, LogD) and acidity (pKa). Nociception was studied in mice either expressing the human NK_1R, which avoided interspecies differences in NK_1R antagonist potency (25), or a truncated human NK_1R that corresponds to a natural variant with aberrant G protein and βARR signaling (26–28). The results show that sustained antagonism of the endosomal NK_1R correlates with long-lasting antinociception, and that domains within the C-terminus of the NK_1R are necessary for the full pronociceptive actions of SP.

Results

SP-Induced Assembly of NK_1R, Gα, and βARR Signalosomes in Early Endosomes. Endosomal signaling of GPCRs is thought to entail the assembly of GPCR, Gα, and βARR signalosomes, where Gα subunits transduce signals and βARRs are scaffolds for GPCRs and signaling enzymes. A bioluminescence resonance energy transfer (BRET) assay was developed to simultaneously study recruitment of the NK_1R and isoforms of Gα or βARR to subcellular compartments of HEK293T cells. Conventional BRET is limited to studying the proximity of only two proteins. To surmount this limitation, NanoLuc Binary Technology BRET (NanoBiT-BRET, nbBRET) was used to simultaneously measure the proximity between the NK_1R, an effector (mini (m) Gα or βARR) plus a localization marker (16, 29) (Fig. 1*A*). mGα proteins are N-terminally truncated Gα proteins that diffuse through the cytosol and bind to active conformations of GPCRs (30, 31); $mG\alpha_{sq}$ and $mG\alpha_{si}$ were developed by mutating $mG\alpha_s$ residues to equivalent $G\alpha_q$ and $G\alpha_i$ residues. NbBRET entails a split luciferase assay in which full-length human NK_1R-407 was C-terminally tagged with the natural peptide fragment of NanoLuc (NP, 13 residue NanoBiT fragment), and a plasma membrane (CAAX) or early endosomal (FYVE) marker was tagged with large NanoBiT fragment (LgBiT). Luminescence occurs from a complex between NK_1R-NP and LgBiT-CAAX or LgBiT-FYVE, which serves as an energy donor for fluorophore-tagged Venus-mGα or βARR-YFP. SP (100 nM) increased nbBRET between NK_1R, $mG\alpha_{sq}$, or βARR2 and LgBiT-CAAX or LgBiT-FYVE, consistent with

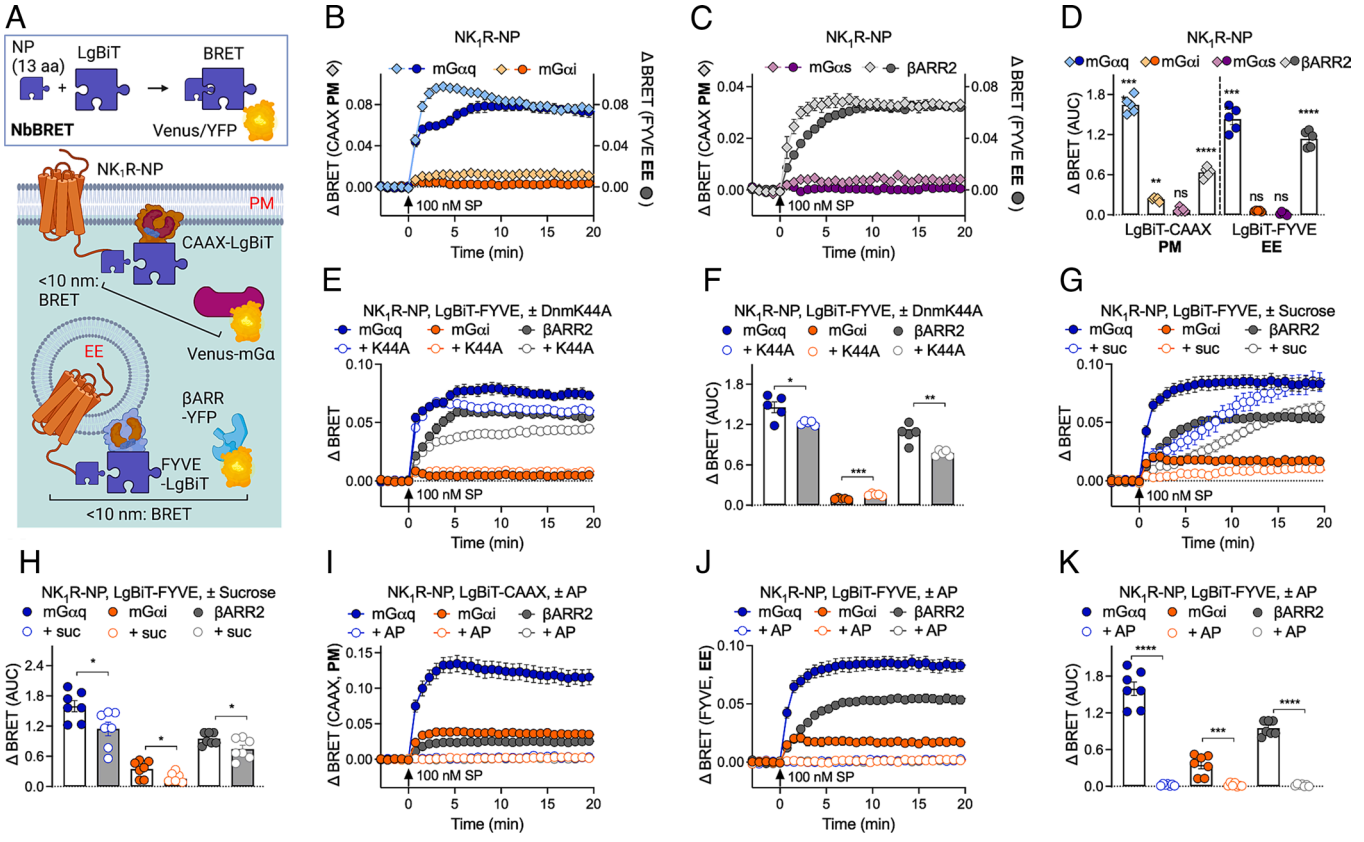

Fig. 1. Assembly of NK_1R signalosomes in HEK293T cells. (*A*) NanoBiT-BRET (nbBRET) uses a nanoluciferase split into two fragments (natural peptide, NP, and LgBiT) to detect BRET between receptor (NK_1R), mini Gα proteins (mGα) or βarrestin (βARR), and proteins resident to the plasma membrane (PM, CAAX) or early endosome (EE, FYVE). (*B–K*) Substance P (SP, 100 nM) induced nbBRET between NK_1R-NP, LgBiT-CAAX, or LgBiT-FYVE as well as Venus-$mG\alpha_{sq}$, Venus-$mG\alpha_{si}$, Venus-$mG\alpha_s$, or βARR2-YFP. (*E–H*) Effect of dominant-negative dynamin (DnmK44A; *E* and *F*) or hypertonic sucrose (0.45 M, 30 min, *G* and *H*). (*I–K*) Effect of aprepitant (AP, 100 nM, 30 min). AUC, area under curve. Mean ± SEM. N = 5 to 7 independent experiments. **P* < 0.05, ***P* < 0.01, ****P* < 0.001, *****P* < 0.0001. One-way ANOVA with Dunnett's test (*D*, *F*, *H*, and *K*).

the recruitment of NK_1R, $mG\alpha_{sq}$, and βARR2 to the plasma membrane and early endosomes (Fig. 1 *B–D*). SP also stimulated a small increase in nbBRET between NK_1R, $mG\alpha_{si}$, and CAAX. Recruitment of $mG\alpha_{sq}$ and βARR2 to early endosomes lagged relative to recruitment to the plasma membrane. Recruitment of NK_1R, $mG\alpha_{sq}$, or βARR2 to the plasma membrane and endosomes was sustained for at least 20 min. Expression of a dominant-negative mutant of dynamin (DnmK44A), which harbors a mutation in the GTPase domain and selectively inhibits receptor endocytosis without affecting protein exocytosis (32), or pretreatment with hypertonic (0.45 M) sucrose, inhibited the recruitment of $NK_1R/mG\alpha_{sq}$, $NK_1R/mG\alpha_{si}$, and $NK_1R/\beta ARR2$ complexes to early endosomes (Fig. 1 *E–H*). Preincubation with the NK_1R antagonist AP (100 nM) abolished complex assembly at the plasma membrane and in early endosomes (Fig. 1 *I–K*).

NK_1R and effector (Gα, βARR) recruitment to intracellular compartments of HEK293T cells was confirmed using conventional BRET assays. To quantify the kinetics of NK_1R trafficking to subcellular compartments, NK_1R-407 tagged with *Renilla* luciferase-8 (Rluc8) was coexpressed with Venus-Kras (plasma membrane marker), Rab5a coupled to tandem *Renilla* green fluorescent protein (tdRGFP, early endosome), Venus-Rab11a (recycling endosome), Venus-Giantin (cis-Golgi network), or YFP-TGN38 (trans-Golgi network) (*SI Appendix*, Fig. S1*A*). SP (100 nM) decreased BRET between NK_1R-Rluc8 and Venus-Kras (*SI Appendix*, Fig. S1 *B* and *C*) and increased BRET between NK_1R-Rluc8 and tdRGFP-Rab5a, Venus-Rab11a, and Venus-Giantin, consistent with NK_1R trafficking from the plasma membrane to early and recycling endosomes and the cis-Golgi network (*SI Appendix*, Fig. S1 *D–I*). BRET between NK_1R-Rluc8 and YFP-TGN38 transiently decreased and then recovered (*SI Appendix*, Fig. S1 *J* and *K*). DnmK44A inhibited NK_1R-Rluc8 recruitment to early endosomes, recycling endosomes and the cis-Golgi network, implicating clathrin-dependent endocytosis. DnmK44A only partially inhibited SP-induced removal of the NK_1R from the plasma membrane, which may reflect the rapid recycling or mobilization of internalized NK_1R, incomplete disruption of endogenous Dnm, or involvement of additional (non-Dnm) mechanisms of receptor endocytosis. DnmK44A caused the BRET signal between NK_1R-Rluc8 and YFP-TGN38 to further decrease, which may implicate Dnm in maintaining a pool of NK_1R within the trans-Golgi network.

Enhanced bystander BRET (ebBRET), which capitalizes on the affinity of protein pairs tagged with *Renilla* fluorophores to improve sensitivity, was used to confirm the recruitment of mGα and βARR2 to the plasma membrane and early endosomes (*SI Appendix*, Fig. S2*A*) (33). EbBRET studies confirmed that SP stimulated recruitment of $mG\alpha_{sq}$, $mG\alpha_{si}$, and βARR2 to the plasma membrane and early endosomes (*SI Appendix*, Fig. S2 *B–G*). BRET between Gγ-GFP and Rluc2-Gα isoforms was measured to study the effects of SP on proximity of Gγ and Gα. SP deceased BRET between Gγ-GFP and Rluc2-$G\alpha_q$ or Rluc2-$G\alpha_i$, consistent with disassembly of the heterotrimeric Gα, Gβ, and Gγ complex or conformational rearrangement of the activated Gα subunit (*SI Appendix*, Fig. S2 *H* and *I*).

Considered together, these results support the hypothesis that SP induces the recruitment of the NK_1R, $mG\alpha_{sq}$, and βARR2 to endosomes, where a multiprotein signalosome may transduce intracellular signals.

Design, Synthesis, and Pharmacological Characterization of NT Analogs. Antagonists were designed to optimally inhibit NK_1R signaling in endosomes. The accumulation and retention of GPCR antagonists in endosomes likely depends on their lipophilicity and charge. Since the lumen of endosomes is acidic (pH 5.5 to 6.0), the degree of ligand protonation may differ between the cytoplasm and endosomal lumen, which could affect endosome membrane penetration and confer enrichment in endosomes and sustained receptor occupancy. Upon receptor binding, the protonation state of the ligand controls association and dissociation and, thus, binding affinity and the kinetic behavior. Furthermore, individual protonation states depending on environment-specific pH values may affect the conformation and, hence, ligand-binding properties of receptors. Ligands were designed with varying lipophilicity (LogP, LogD) and acidity (pKa) to promote accumulation or to take advantage of a potentially altered receptor conformation in endosomes at sufficient concentrations to extend the residence time at the endosomal NK_1R. To determine the criteria for design of antagonists of endosomal GPCRs, a series of structural analogs of the NK_1R antagonist NT ("PS" series) were developed. NT caused a concentration-dependent inhibition of $mG\alpha_{sq}$ recruitment to NK_1R-NP at the plasma membrane and in early endosomes (Fig. 2 *A–C*). NT had a lower potency in early endosomes (NT, FYVE pIC_{50} 7.70 ± 0.12, n = 5) compared to the plasma membrane (NT, CAAX pIC_{50} 8.19 ± 0.17, n = 5; unpaired *t* test, $P < 0.05$).

To better understand NT structure–activity relationships, the weakly basic pyridine nitrogen was replaced with a benzene ring (34) (Fig. 2 *D–G*). Initial investigations were directed to the synthesis and pharmacological investigation of carba-NT (PS15) with only one basic nitrogen. Further ligand modifications were guided by the crystal structure of the NT/NK_1R complex (PDB ID: 6HLP), which revealed that the $N(CH_3)$ group of the piperazine ring is ideally suited for further modifications (35). Examination of the binding pocket and subsequent docking studies indicated that a replacement of the $N(CH_3)$ group by O or CH_2 is possible, and the introduction of even large N-substituents is well tolerated. Hence, a series of carba-NT derivatives were synthesized to enable introduction of neutral (PS9, PS29), acidic (PS34), weakly basic (PS40), basic (PS21), and strongly basic (PS49) groups (Fig. 2*G* and Table 1). A maleimide group (PS26) was introduced to enable formation of a covalent bond to the NK_1R. Fluorescent tetramethylrhodamine (TAMRA) derivatives of NT were also prepared (PS67, PS68, PS69). Based on the preparation of NT (36), synthesis started from 2-bromo-4-fluoronitrobenzene to generate a biphenyl system using a Suzuki reaction (*SI Appendix*). Nucleophilic aromatic substitution allowed introduction of different saturated heterocyclic moieties. Reduction of the nitro group, *N*-methylation, and amide coupling reaction resulted in the introduction of a 1,3-bistrifluoromethylphenyl substituted isobutyric acid moiety and thus, final product formation. To characterize their binding affinity (K_d) at NK_1R, a BRET-based assay was developed using membranes from HEK293T cells expressing human NK_1R tagged at the N terminus with nanoluciferase (Nluc) and TAMRA-NT (*SI Appendix*, Fig. S3). Binding was measured at normal extracellular pH 7.4 or the acidic pH 6.0 of endosomes. At pH 7.4, TAMRA-NT analogs showed high affinities for Nluc-NK_1R (PS68, K_d 1.9 ± 0.39 nM, n = 12; PS69, K_d 0.81 ± 0.065 nM, n = 21). PS69 was then used as a fluorescent tracer to determine the affinity of SP (K_i 1.4 ± 0.46 μM, n = 6). The orthosteric NK_1R antagonists AP and NT inhibited binding with K_i values of 0.15 nM and 0.91 nM, respectively (Table 1). At pH 7.4, PS analogs retained binding with K_i values ranging from 0.72 nM (PS15) to 110 nM (PS21). Each NT analog also had nanomolar affinity for NK_1R at acidic pH 6.0, thus retaining the ability to antagonize SP/NK_1R binding in acidic endosomes. Most of the compounds showed slightly diminished binding affinities in the acidified environment. An approximately 2-fold and 20-fold increase in affinity was observed for weakly basic

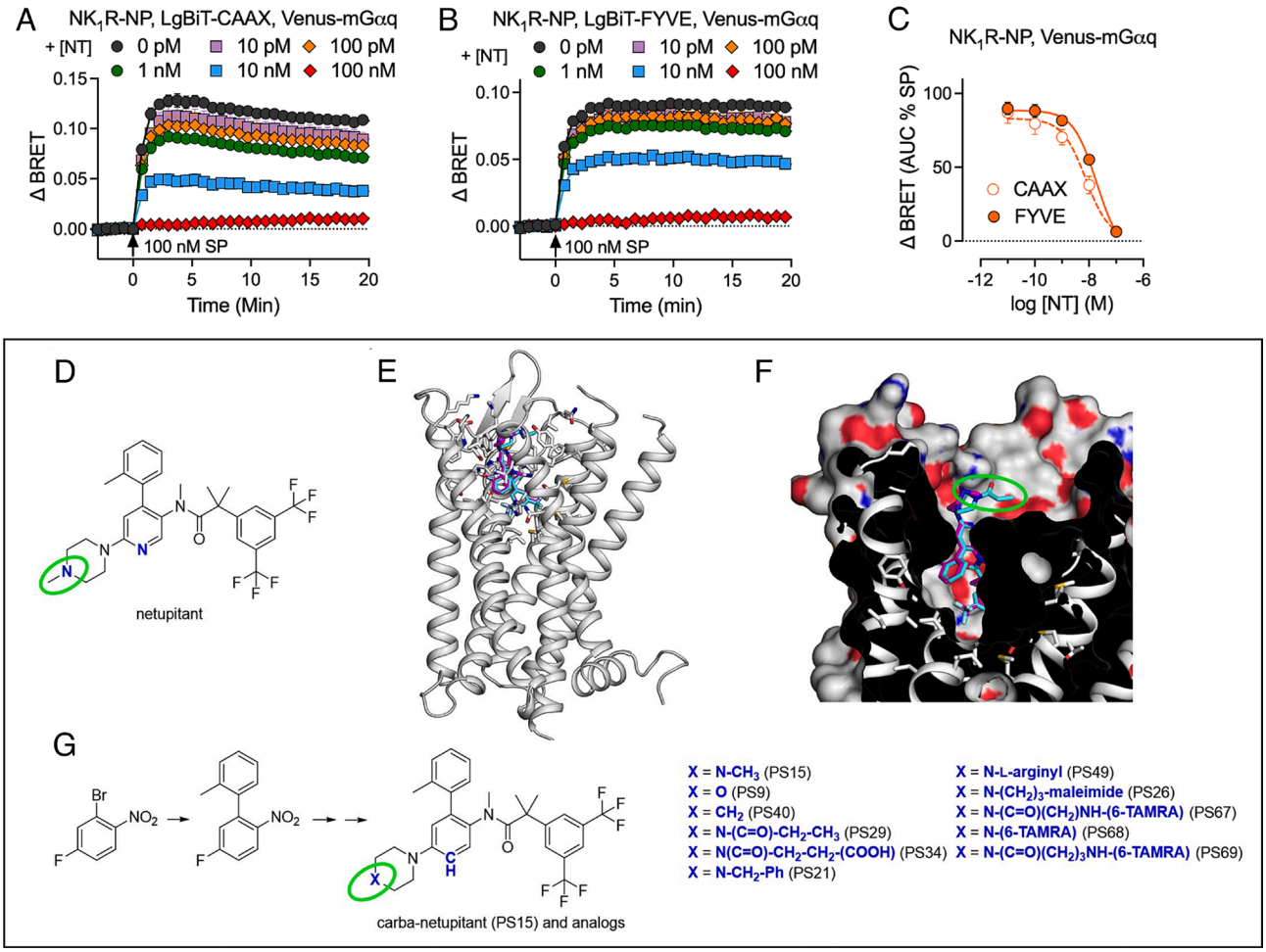

Fig. 2. Development of netupitant analogs. (*A–C*) Effect of graded concentrations of netupitant (NT, 30 min) on substance P (SP)–induced recruitment of mini $G\alpha_{sq}$ (mGαq) to the plasma membrane (CAAX, *A*) or early endosome (FYVE, *B*) on NanoBiT-BRET (nbBRET) with natural peptide (NP)–tagged NK_1R in HEK293T cells. (*D–G*) Design and synthesis of NT analogs. (*D*) Chemical formula of NT. (*E*) NK_1R crystal structure (PDB ID: 6HLP) in complex with NT (magenta) overlaid with the docked pose of PS29 (blue). Residues are displayed in a range of 8 Å relative to NT and PS29. F. NT (PDB ID: 6HLP) in complex with the NK_1R crystal structure (PDB ID: 6HLP) presented together with the docked pose of PS29. Receptor surface is clipped between the transmembrane helices 4, 5, and 6 to give better insight into the binding pocket and to show the outward reaching piperazine substituent of NT and PS29 (green circle), showing surface atoms and hetero atoms [oxygen (red), nitrogen (blue), sulfur (yellow)]. (*G*) Synthetic approach toward carba-NT derivatives. Structural changes compared to NT are highlighted in blue. Mean ± SEM. N = 4 to 9 independent experiments.

arylpiperidine PS40 [K_i (pH 7.4) = 71 nM; K_i (pH 6.0) = 36 nM] and the lipophilic and basic benzylamine PS21 [K_i (pH 7.4) = 110 nM; K_i (pH 6.0) = 4.4 nM], respectively, indicating that protonation affects ligand binding.

Inhibitory Actions of NK_1R Antagonists on SP-Induced Endosomal Signaling. The potency of NT analogs was determined by measuring inhibition of SP-induced inositol 1-phosphate (IP_1) accumulation. SP potently stimulated IP_1 accumulation (SP, EC_{50} 5.1 ± 1.1 nM, n = 8). To quantify antagonist potency (IC_{50}), HEK293T cells expressing the human NK_1R were preincubated with antagonists (90 min), challenged with SP (10 nM, ~EC_{80}, 90 min), and IP_1 accumulation was assessed. AP and NT inhibited SP-stimulated IP_1 accumulation with IC_{50} values of 170 nM and 178 nM, respectively (Table 1). PS analogs retained activity with IC_{50} values ranging from 91 nM (PS21) to 407 nM (PS49).

To evaluate whether NK_1R antagonists inhibit endosomal signaling, a Förster resonance energy transfer (FRET) biosensor targeted to the nucleus (Nuc-EKAR) was used to measure nuclear ERK activity, which emanates from NK_1R signaling in endosomes (9). HEK293T cells cotransfected with human NK_1R and NucEKAR were preincubated (30 to 90 min) with graded concentrations of NK_1R antagonists and challenged with SP (10 nM, ~ EC_{50}; *SI Appendix*, Fig. S2*J*). NT caused a concentration-dependent inhibition of SP-induced nuclear ERK activity (Fig. 3*A* and Table 1). NT was less potent than AP (Fig. 3*B*; NT, pIC_{50} 6.59 ± 0.12; AP, pIC_{50} 6.94 ± 0.17; n = 4 to 6). PS analogs with different physicochemical properties induced concentration-dependent inhibition of SP-induced activation of nuclear ERK with comparable potency (Fig. 3*C* and Table 1; pIC_{50} 6.16 to 6.72).

To determine the duration of antagonism (approximating to k_{off}), cells were preincubated with antagonists (30 to 90 min), washed, recovered for 2 or 4 h, and then challenged with SP. Most of the inhibitory effect of AP was lost within 2 h of recovery and is thus transient (Fig. 3 *D* and *E* and Table 1). In contrast, the inhibitory effects of NT and PS analogs were largely maintained after recovery for 2 h (Fig. 3 *D* and *E*) and 4 h, respectively (Fig. 3*F* and *SI Appendix*, Fig. S4 *A–F*). These results were consistent for two antagonist concentrations (*SI Appendix*, Fig. S4 *A–F*).

To assess the kinetics with which antagonists reverse endosomal NK_1R signaling (approximating to k_{on}), SP-evoked recruitment of mGα to early endosomes was studied by measuring ebBRET between Rluc8-$mG\alpha_{sq}$ and tdRFP-Rab5a. Cells were incubated

Table 1. Pharmacological properties of NK_1R antagonists

	Compound properties					Binding affinity		Potency of inhibition		Kinetics of inhibition
	Derived*, † or calculated‡, §					BRET (Nluc-NK_1R)¶		IP_1 (HTRF)	Nuclear ERK (FRET)	Endosomal mini$G\alpha_{sq}$ (ebBRET)
	pKa*	pKa‡	LogP§	$LogD_{5.0}$†	$LogD_{7.0}$†	pK_i at pH 7.4	pK_i at pH 6.0	pIC_{50}	pIC_{50}	k (min^{-1}) for 10 μM
AP (neutral)	n.d.	n.d.	n.d.	n.d.	n.d.	9.82 ± 0.08 (5)	9.27± 0.06 (3)	6.77 ± 0.17 (4)	6.94 ± 0.17 (4)	0.15 ± 0.01 (4)
NT (basic)	6.81	6.51	7.22	n.d.	4.97	9.04 ± 0.07 (5)	9.07 ± 0.08 (3)	6.75 ± 0.10 (10)	6.59 ± 0.12 (6)	0.14 ± 0.02 (9)
PS15 (carba-NT)	6.95	7.44	7.54	3.85	5.06	9.14 ± 0.07 (4)	8.59 ± 0.04 (3)	6.50 ± 0.13 (5)	6.38 ± 0.09 (4)	0.23 ± 0.04 (9)
PS9 (neutral)	<3	2.23	7.66	n.d.	3.49	8.84 ± 0.08 (3)	8.45 ± 0.05 (3)	6.87 ± 0.07 (4)	6.29 ± 0.09 (4)	0.11 ± 0.04 (5)
PS40 (weakly basic)	4.31	4.13	8.73	n.d.	n.d.	7.15 ± 0.08 (4)	7.45 ± 0.12 (3)	6.78 ± 0.14 (7)	6.22 ± 0.15 (4)	n.d. – slow kinetics
PS29 (neutral)	<3	1.27	7.37	5.05	4.99	8.73 ± 0.07 (3)	8.31 ± 0.08 (5)	6.84 ± 0.18 (5)	6.46 ± 0.21 (4)	0.14 ± 0.02 (5)
PS21 (basic)	6.17	6.21	9.30	Not trace-able log D >> 5	Not trace-able log D >> 5	6.96 ± 0.02 (3)	8.36 ± 0.07 (3)	7.04 ± 0.11 (4)	6.50 ± 0.25 (4)	n.d. – slow kinetics
PS49 (basic)	>10	11.55	5.45	n.d.	n.d.	8.44 ± 0.08 (4)	7.59 ± 0.08 (6)	6.39 ± 0.09 (5)	6.36 ± 0.16 (5)	0.21 ± 0.01 (7)
PS34 (acidic)	n.d.	6.11	6.41	4.90	3.49	8.74 ± 0.03 (3)	8.69 ± 0.08 (5)	6.75 ± 0.11 (6)	6.16 ± 0.09 (5)	0.11 ± 0.01 (7)
PS26 (covalent)	n.d.	9.16	7.50	n.d.	n.d.	8.64 ± 0.08 (3)	7.91 ± 0.06 (3)	6.68 ± 0.17 (5)	6.72 ± 0.30 (4)	0.11 ± 0.02 (5)

*Free base titrated in 67% MeOH in H_2O (0.01 M HCl).
†LogD experiments with distribution between octanol and aqueous buffer solution at pH 5.0 and pH 7.0. n.d. not determined.
‡Calculated with Jaguar (Maestro Schroedinger).
§Calculated with QikProp (Maestro Schroedinger).
¶Determined by competition binding with fluorescent TAMRA-NT (PS69).

with SP (10 nM) for 5 min and then treated with NK_1R antagonists or vehicle (Fig. 3*G*). SP stimulated recruitment of $mG\alpha_{sq}$ to early endosomes that was maintained for at least 40 min. AP, NT, and PS analogs caused a concentration-dependent inhibition of $mG\alpha_{sq}$ recruitment, reaching equilibrium by 40 min (*SI Appendix*, Fig. S5). At a saturating concentration, PS15 induced a rapid disruption of the endosomal signal within 15 min, with a faster rate than AP, NT, or other analogs (Fig. 3 *G* and *H* and Table 1).

To evaluate the uptake of NT, HEK293T cells transiently expressing NK_1R-eGFP were incubated with TAMRA-NT (100 nM) and imaged using confocal microscopy. TAMRA-NT was taken up into cells within minutes regardless of NK_1R-eGFP expression (Fig. 3*I* and Movie S1). TAMRA-NT also colocalized with NK_1R-eGFP at the plasma membrane. Preincubation with SP prevented TAMRA-NT binding to NK1R-eGFP at the plasma membrane (Fig. 3*I* and Movie S2).

Thus, NT analogs penetrate cells and disrupt endosomal NK_1R signaling. Whereas the inhibitory actions of AP are rapidly reversed, NT analogs are long lasting and persist after washing cells to remove ligand.

Generation of Knockin Mice Expressing Full-Length hNK_1R-407 or Truncated hNK_1R-311. Differences in the potency of antagonists between human and mouse NK_1R, including for AP and NT, significantly hamper studies of the NK_1R in preclinical disease models (25). To circumvent this problem, knockin mice were generated in which the mouse NK_1R was replaced by the full-length human NK_1R (407 residues). A naturally occurring variant of the NK_1R has been described in several species, including human, that is truncated at residue 312 and lacks most of the intracellular C-terminal domain (26–28). To examine the function of this variant, knockin mice were generated in which mouse NK_1R was replaced by the truncated human variant (311 residues). This variant binds SP but displays diminished G protein signaling, interaction with βARRs, and internalization (9, 27). Thus, a comparison of SP-evoked nociception in NK_1R-407 and NK_1R-311 mice could give insight into the contribution of NK_1R endosomal signaling to pain.

Targeting constructs were designed to express tdTomato reporter (to detect NK_1R-expressing cells), a 2A peptide (cleavage would liberate tdTomato), and Flag-NK_1R-407 or Flag-NK_1R-311 (Fig. 4*A* and *SI Appendix*, Fig. S6*A*). Constructs were generated by homologous recombination using a 10 kb segment of mouse genomic DNA from a C57 BAC clone. Synthetic cDNAs encoding NK_1R-407 or NK_1R-311 were codon optimized for mouse. tdTomato followed by a 2A peptide was incorporated upstream and a neomycin cassette flanked by FRT sites was incorporated downstream from the NK_1R cDNAs. The cassette was inserted at the ATG site of mouse NK_1R and the first exon was deleted. Constructs were linearized and electroporated in Bruce4 (C57BL/6) ES cells. Screening of 200 clones revealed 8 to 14% ratio of recombination, which was confirmed by southern blotting (Fig. 4*B* and *SI Appendix*, Fig. S6*B*). Clones were analyzed using an internal probe annealing on the NEO cassette (Fig. 4*C* and *SI Appendix*, Fig. S6*C*). Sequencing of five NK_1R-407 and five NK_1R-311 clones confirmed correct insertion of tdTomato and integrity of FRT sites. Three clones were injected into mouse blastocysts, and male chimeras (black and white) were bred with wild-type C57BL/6 female mice to generate black F1 progeny; two clones gave germline transmission. Expression of NK_1R-407 and NK_1R-311 was confirmed by southern blotting of the heterozygotic F1 generation (Fig. 4*D* and *SI Appendix*, Fig. S4*D*) and RT-PCR of knockin mice. F1 mice were backcrossed for >10 generations to generate homozygotic NK_1R-407 and NK_1R-311 mice.

Characterization of hNK_1R-407 and hNK_1R-311 Mice. The expression of the NK_1R was verified in hNK_1R-407, hNK_1R-311, and wild-type mice using PCR and qRT-PCR with primers for mouse (m) or human (h) receptors, including primers specific to hNK_1R-407 but not hNK_1R-311 and primers that would

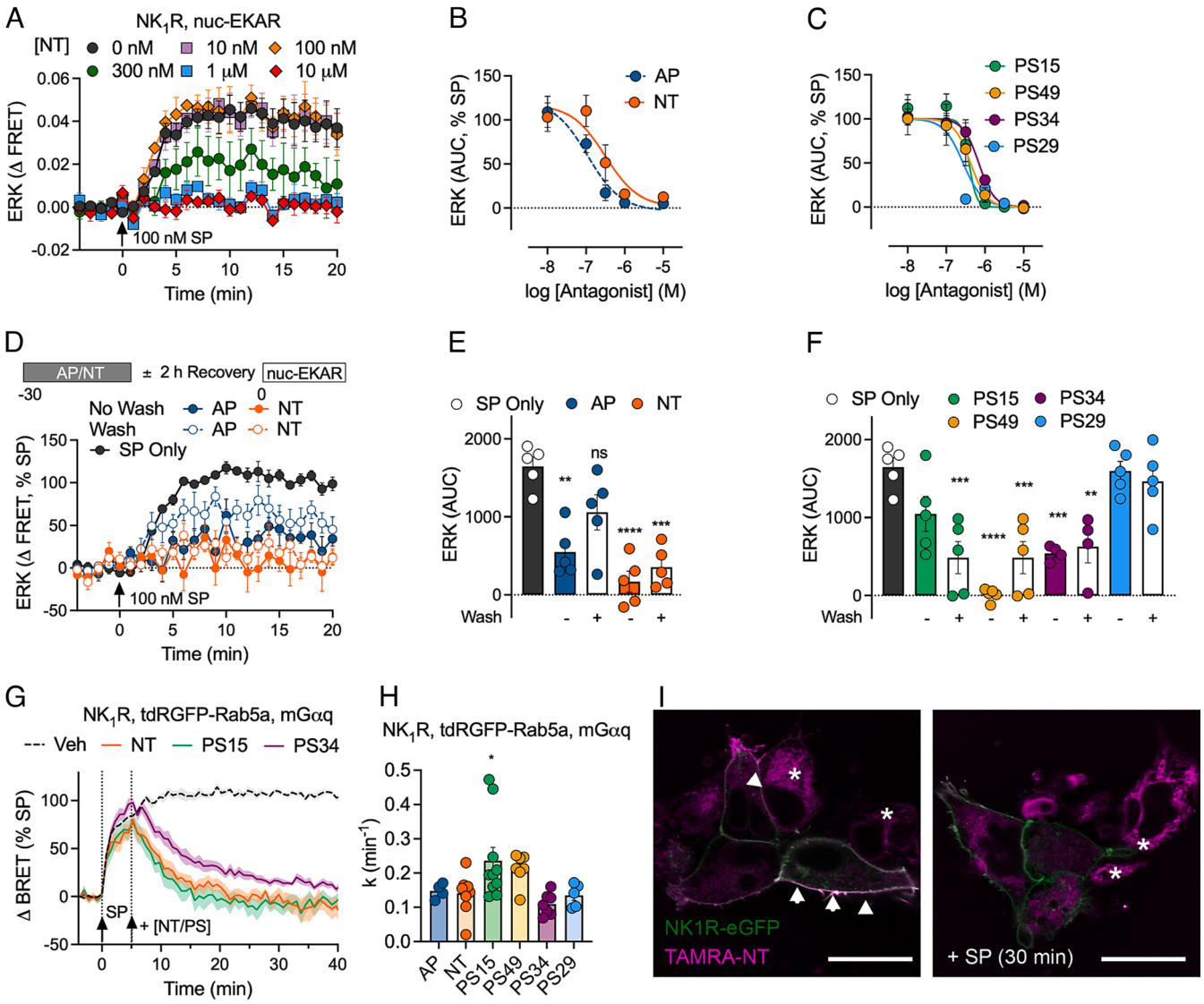

Fig. 3. Antagonism of NK_1R endosomal signaling in HEK293T cells. (*A–F*) FRET assays of substance P (SP)–induced activation of nuclear ERK activity measured using a nuclear EKAR biosensor. (*A–C*) Cells were preincubated (30 or 90 min) with graded concentrations of aprepitant (AP), netupitant (NT), PS15, PS29, PS34, or PS49 prior to SP (100 nM) challenge. (*D–F*) Duration of inhibition following antagonist removal and recovery. Cells were preincubated with antagonist for 30 min (AP, 100 nM; NT, 300 nM) or 90 min (NT analogs, 1 µM), washed, and recovered in agonist-free medium for 2 h (AP, NT) or 4 h (NT analogs; *SI Appendix*, Fig. S3), prior to stimulation with SP (100 nM). (*G* and *H*) Enhanced bystander BRET (ebBRET) measuring proximity between mini $G\alpha_{sq}$ (Venus-$mG\alpha_{sq}$) and a *Renilla* luciferase–tagged endosomal marker (tdRGFP-Rab5a). Cells were stimulated with SP (100 nM, 5 min), then challenged with vehicle or saturating concentrations of NT, PS15, or PS34 (10 µM). EbBRET was measured for 40 min. Kinetics were fitted as a nonlinear exponential decay from antagonist addition to quantify the rate of antagonism. Mean±SEM. N = 4 to 9 independent experiments. 1-way ANOVA with Holm-Šídák's (*E*), Dunnett's (*F*) test against SP, or Dunnett's against NT (*H*). (*I*) Localization of fluorescent TAMRA-NT (PS68, 100 nM, 10 min, magenta) in HEK293T cells expressing NK_1R-eGFP (green), with or without preincubation with unlabeled SP (100 nM, 30 min). Arrow heads denote TAMRA-NT and NK_1R-eGFP colocalization at the plasma membrane. Asterisks denote uptake of TAMRA-NT into cells lacking NK_1R-eGFP. (Scale bar, 20 µm). Representative images, N = 3 experiments.

detect both hNK_1R-407 and hNK_1R-311. Primers specific to hNK_1R-407 detected the receptor in extracts of the spinal cord and colon from hNK_1R-407 mice, but not hNK_1R-311 or wild-type mice (Fig. 5 *A–C*). Primers common to hNK_1R-407 and hNK_1R-311 detected both receptors at similar levels in the spinal cord and colon of hNK_1R-407 and hNK_1R-311 mice but not in wild-type mice.

RNAScope® in situ hybridization was used to localize human and mouse NK_1R mRNAs in the spinal cord of mice. Probes were designed to specifically target both human NK_1R-407 and NK_1R-311 or mouse NK_1R. Neurons were identified by Nissl staining. Corroborating with the qRT-PCR results, a probe common to human NK_1R-407 and NK_1R-311 hybridized to spinal neurons of hNK_1R-407 and hNK_1R-311 but not in wild-type mice (Fig. 5*D*). Mouse NK_1R mRNA was detected in spinal neurons of wild-type mice (Fig. 5*D*).

SP-Evoked Nociception in hNK_1R-407 or hNK_1R-311 Mice. Since NK_1R-311 displays aberrant signaling by G proteins and βARRs and is resistant to SP-induced endocytosis (9, 27, 37), a comparison of the pronociceptive actions of SP between mice expressing full-length or truncated human NK_1R could provide insights into the contribution of NK_1R signaling and endocytosis to nociception. SP (0.1, 1, 3 µg/5 µL) was injected intrathecally to activate spinal neurons expressing the NK_1R in hNK_1R-407, hNK_1R-311, and wild-type mice. Paw withdrawal responses to stimulation with von Frey filaments were assessed over 1 h to evaluate mechanical allodynia. SP dose-dependently reduced withdrawal threshold

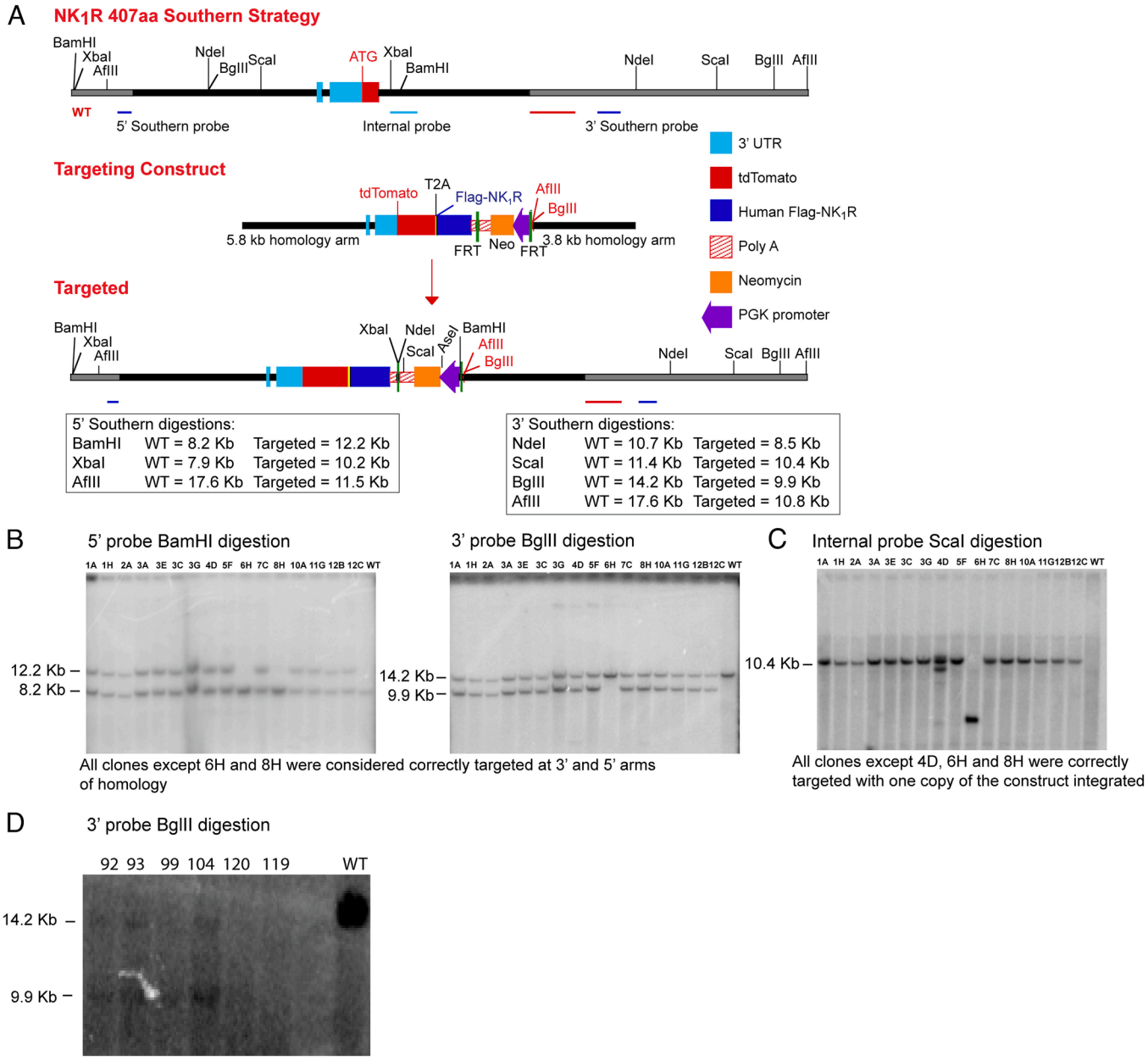

Fig. 4. Generation of knockin mice expressing hNK$_1$R-407. (*A*) NK$_1$R-407 Southern strategy and targeting construct comprising tdTomato, a T2A peptide cleavage site, Flag-hNK$_1$R-407, a downstream phosphoglycerine kinase neomycin cassette flanked by FRT sites, and downstream AflII and BglII sites. (*B* and *C*) Southern blots of selected clones with 5′, 3′, and internal probes confirming correct targeting. (*D*) Southern blot of F1 mice confirming NK$_1$R-407 expression. WT, wild-type.

to von Frey filaments in hNK$_1$R-407, hNK$_1$R-311, and wild-type mice, consistent with mechanical allodynia (Fig. 6 *A*–*C*). All doses of SP evoked mechanical allodynia, which was detected after 15 min, was maximal at 30 min, and returned to baseline at 60 min after injection. A comparison of mechanical allodynia between strains to the same dose of SP indicated identical mechanical allodynia in hNK$_1$R-407 and wild-type mice to all doses of SP (Fig. 6 *D*–*I*). Mechanical allodynia in hNK$_1$R-311 mice was less than that in NK$_1$R-407 and wild-type mice at all doses of SP, and this difference was significant at 1 μg SP (Fig. 6 *E* and *H*).

Although SP is the primary ligand for the NK$_1$R, SP can also activate the NK$_2$R and NK$_3$R, albeit with low affinity (25). To confirm that the SP nociceptive response was dependent on the NK$_1$R, AP (100 nM/5 μL) was coadministered with SP (1 μg/5 μL) by intrathecal injection. AP abolished SP-evoked mechanical allodynia in hNK$_1$R-407, hNK$_1$R-311, and wild-type mice (Fig. 6 *J* and *K*).

SP activates the NK$_1$R on spinal neurons to evoke receptor endocytosis and persistent neuronal excitation. Inhibitors of clathrin-mediated endocytosis, and lipidated or nanoparticle-encapsulated NK$_1$R antagonists that target endosomes, prevent sustained neuronal excitation, which thus requires NK$_1$R signaling in endosomes (9, 17). To obtain further evidence for the contribution of NK$_1$R endocytosis to nociception, spinal cord slices from NK$_1$R-407 and NK$_1$R-311 mice were superfused with SP (10 nM, 2 min), and action potential firing was assessed by cell-attached patch-clamp recording. SP induced a rapid-onset burst of action potential discharge that was similar in spinal neurons of NK$_1$R-407 and NK$_1$R-311 (Fig. 6 *L*–*N*). In NK$_1$R-407 mice, neuronal excitation persisted for 12 min after SP washout. In contrast, in NK$_1$R-311 mice, neuronal excitation returned to baseline by 4 min after SP

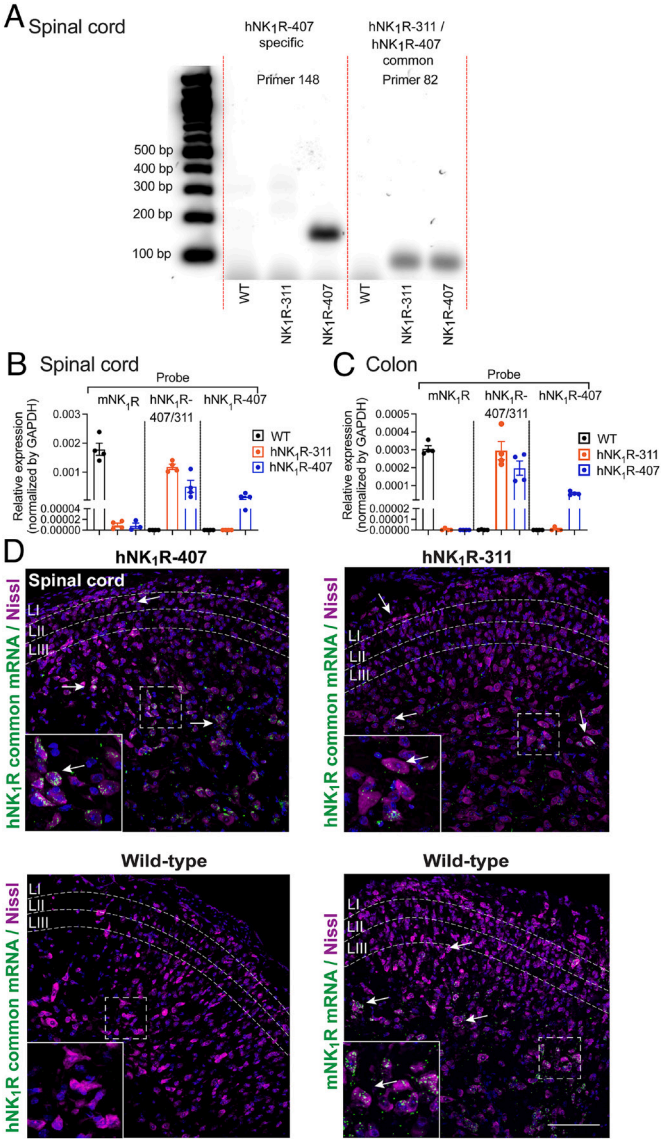

Fig. 5. Characterization of mice expressing hNK$_1$R-407 or hNK$_1$R-311. (*A*) PCR gels of the spinal cord from NK$_1$R-407, NK$_1$R-311, and WT mice probed with a primer (#148) specific for human NK$_1$R-407 or a primer (#82) that would detect both human NK$_1$R-407 and NK$_1$R-311. (*B* and *C*) qRT-PCR analysis of extracts of the spinal cord (*B*) and colon (*C*) probed with primers to mouse NK$_1$R, both human NK$_1$R-407 and NK$_1$R-311, or hNK$_1$R-407 alone. N = 4 mice. (*D*) RNAScope® in situ hybridization of sections of the spinal cord from NK$_1$R-407, NK$_1$R-311, or WT mice using probes to both human NK$_1$R-407 and NK$_1$R-311 or to mouse NK$_1$R, highlighting neurons with a Nissl stain (magenta). Representative images from n = 3 mice. Scale bar, 50 μm, and in detail box, 20 μm. L, lamina.

washout. AP prevented SP-induced excitation of spinal neurons in NK$_1$R-407 mice.

Attenuated SP-induced activation of spinal neurons and diminished nociception observed in mice expressing truncated NK$_1$R support the hypothesis that efficient coupling to G proteins, βARRs, and the endocytic machinery are necessary for SP-evoked pain.

Antinociceptive Effects of NK$_1$R Antagonists in hNK$_1$R-407 Mice. To assess whether effective antagonism of NK$_1$R signaling in endosomes correlates with antinociceptive activity, the effect of NK$_1$R antagonists was evaluated on capsaicin-induced mechanical allodynia in hNK$_1$R-407 mice. AP, NT, NT analogs (PS15, PS29, PS34, PS49) (10, 30, 100 or 300 nM, 5 μL) or vehicle (control) was injected intrathecally immediately before intraplantar injection of capsaicin. Withdrawal responses of the capsaicin-injected (right, ipsilateral) hindpaw to stimulation with von Frey filaments were assessed to evaluate mechanical allodynia. In vehicle-treated mice, capsaicin caused mechanical allodynia for 8 h (Fig. 7 A and B). Intrathecal AP (100 nM) inhibited capsaicin-evoked mechanical allodynia for 2 h. NT (100 nM) inhibited mechanical allodynia for 4 h. PS15, PS29, PS34, and PS49 (100 nM) had more efficacious and sustained antinociceptive effects. PS29 and PS34 completely prevented capsaicin-evoked mechanical allodynia for 4 h, with antinociceptive effects for at least 8 h. Higher doses of AP or NT (300 nM) did not further increase the magnitude or duration of the antinociception (Fig. 7 *C*, *D*, and *F*). In contrast, lower doses of PS34 (30 nM) still induced antinociception for 6 h. Thus, NT analogs that effectively inhibit endosomal signaling of the NK$_1$R also caused efficacious and persistent antinociception.

Discussion

The results support the hypothesis that SP stimulates recruitment of the NK$_1$R, mGα$_{sq}$, mGα$_{si}$, and βARR2 to early endosomes, where an NK$_1$R, mGα, and βARR signalosome may assemble and generate signals in subcellular compartments, including ERK activation in the nucleus. Although AP, NT, and NT analogs can disrupt complex formation and inhibit resultant signals, the actions of AP are rapidly reversed. NT analogs, in particular PS29 and PS34, demonstrate sustained antagonism of endosomal signaling and potent, efficacious, and long-lasting inhibition of nociception in mice expressing the human NK$_1$R. In mice expressing a truncated NK$_1$R variant with aberrant signaling and endosomal trafficking, SP is unable to cause sustained activation of spinal neurons and persistent nociception. The results identify criteria for the design of GPCR antagonists that are capable of penetrating endosomes and disrupting signalosomes and provide evidence for the contribution of endosomal NK$_1$R signaling in nociception.

NK$_1$R Signalosomes in Endosomes. BRET assays of NK$_1$R trafficking revealed that SP induces depletion of NK$_1$R from the plasma membrane and recruitment to early endosomes, recycling endosomes, and the Golgi apparatus. NK$_1$R trafficking was Dnm dependent because dominant-negative Dnm inhibited NK$_1$R endocytosis and accumulation in endosomes and the cis-Golgi apparatus. SP also stimulated the recruitment of mGα$_{sq}$, mGα$_{si}$, and βARR2, but not mGα$_s$, to the plasma membrane and early endosomes. A nbBRET assay allowed simultaneous evaluation of the proximity of the NK$_1$R, an effector (mGα, βARR2), and a plasma membrane or endosomal marker. These studies suggest that SP evokes assembly of NK$_1$R signalosomes with mGα$_{sq}$, mGα$_{si}$, or βARR2 in early endosomes. Although BRET assays can be used to infer signalosome assembly, the approach evaluates protein proximity rather than interaction. However, structural studies support the concept that GPCRs could physically associate with Gα and βARRs in endosomes, forming "megaplexes" that continue to signal (12, 13). GPCR signalosomes in endosomes generate second messengers and activate enzymes in specific intracellular compartments, including nuclear ERK and cytosolic protein kinase C and cAMP in the case of the NK$_1$R (9). Compartmentalized signals allow GPCRs, which often couple to a common set of effectors, to regulate specific cellular functions, including activity of spinal neurons that is required for the central transmission of pain (9). Further studies are required to evaluate the physiological relevance of recruitment of the NK$_1$R and isoforms of Gα and βARRs to endosomes, including stimulation of cells that endogenously express these proteins with biologically relevant concentrations of SP.

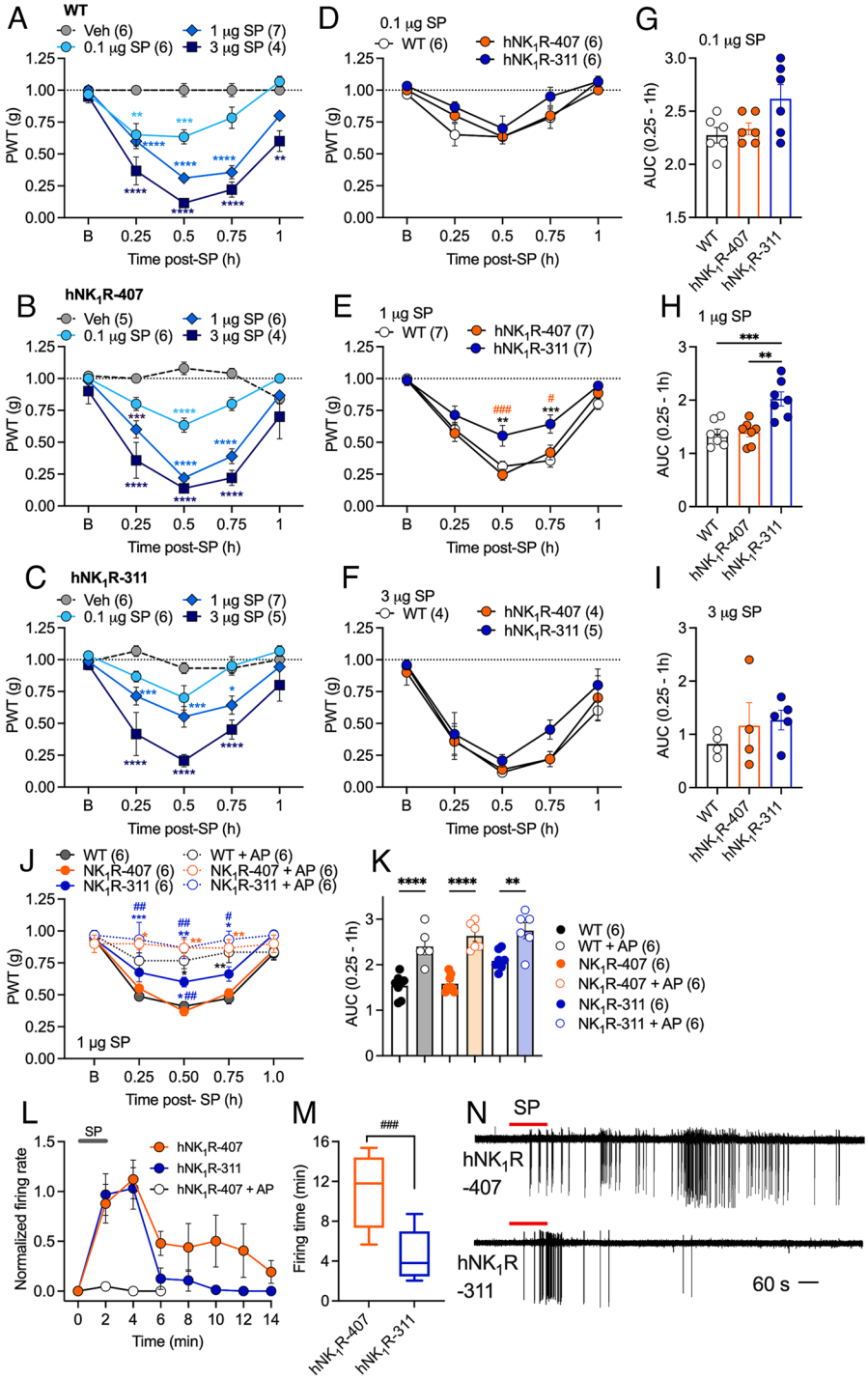

Fig. 6. SP-evoked nociception in hNK$_1$R-407, hNK$_1$R-311, and wild-type mice. (*A*–*C*) Substance P (SP; 0.1, 1, 3 µg/5 µL, intrathecal)–evoked mechanical allodynia in WT (*A*), NK$_1$R-407 (*B*), and NK$_1$R-311 (*C*) mice. Mechanical allodynia was measured 0.25 to 1 h after SP injection. (*D*–*F*) Mechanical allodynia to the same dose of SP in the three strains of mice. Paw withdrawal threshold (PWT) to stimulation with calibrated von Frey filaments was measured to assess mechanical allodynia. (*G*–*I*) AUC in the three strains of mice. (*J* and *K*) Effects of intrathecal injection of aprepitant (AP, 100 nM/5 µL) or vehicle on SP (1 µg/5 µL)-evoked mechanical allodynia in NK$_1$R-407, NK$_1$R-311, and WT mice. (*L*–*N*) Activation of spinal neurons in slice preparations of spinal cord from NK$_1$R-407 and NK$_1$R-311 mice after transient stimulation with SP (10 nM, 2 min). (*L*) Normalized firing rate. (*M*) Firing time. (*N*) Representative traces. Mean ± SEM; (N) denotes number of mice studied. $^*P < 0.05$, $^{**}P < 0.01$, $^{***}P < 0.001$, $^{****}P < 0.0001$ vs. Veh, WT; $^{\#}P < 0.05$, $^{\#\#}P < 0.01$, $^{\#\#\#}P < 0.001$ vs. NK$_1$R-407. Two-way ANOVA, Sídák's multiple comparison test (*A*–F and *J*), one-way ANOVA, Tukey's multiple comparison test (*G*–*I* and *K*), or parametric unpaired two-tailed *t* test (*M*).

Antagonism of NK$_1$R Signaling in Endosomes. Whereas GPCR signaling at the plasma membrane is tightly regulated by GRK-mediated receptor phosphorylation and interaction with βARRs, GPCR signaling in endosomes is often sustained. The mechanisms that terminate endosomal signaling are not fully understood. However, degradation of SP in acidic endosomes by the transmembrane peptidase endothelin–converting enzyme 1 disrupts signalosomes and terminates endosomal signaling of the NK$_1$R (38, 39). The observations that inhibitors of endocytosis block compartmentalized signaling and nociception provide a link between endosomal signaling and pain and suggest that GPCRs in endosomes are an optimal target for the treatment of pain (9, 11, 16). GPCR antagonists conjugated to the transmembrane lipid cholestanol or encapsulated into nanoparticles accumulate in early

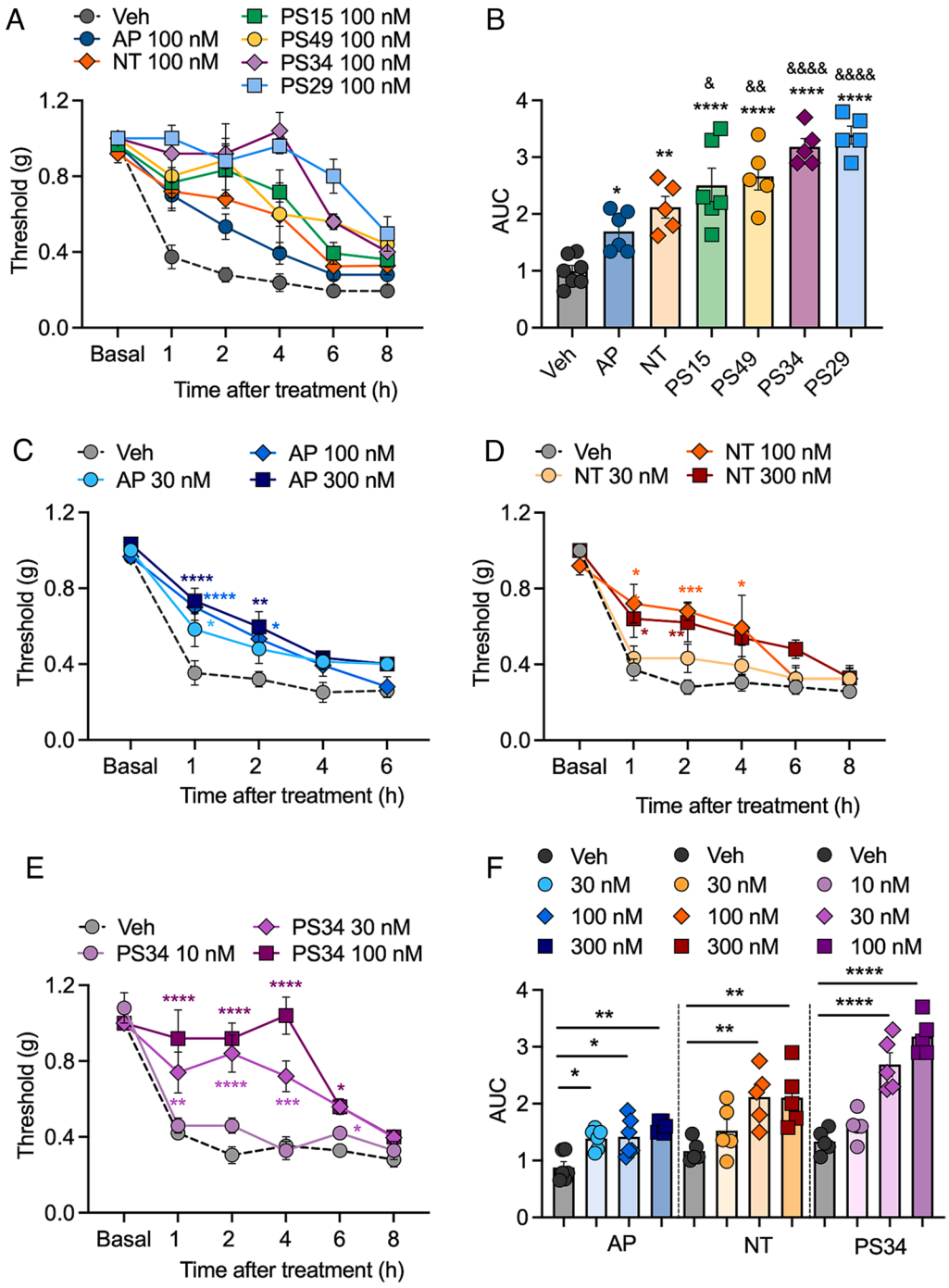

Fig. 7. Antagonism of capsaicin-evoked nociception in hNK_1R-407 mice. (*A*) Effects of intrathecal (i.t.) injection of aprepitant (AP), netupitant (NT), or NT analogs (PS15, PS49, PS34, PS29; 100 nM/5 µL) on capsaicin-induced mechanical allodynia in hNK_1R-407 mice. (*B*) AUC in the same groups of mice. (*C–E*) Dose–response effects of AP (30, 100, 300 nM/5 µL, i.t.), NT (30, 100, 300 nM/5 µL, i.t.), or PS34 (10, 30, 100 nM/5 µL, i.t.) on capsaicin-induced mechanical allodynia. (*F*) AUC in the same groups of mice. (N) denotes number of mice studied. $^{*}P < 0.05$, $^{**}P < 0.01$, $^{***}P < 0.001$, $^{****}P < 0.0001$ vs. Veh; $^{\&}P < 0.05$, $^{\&\&}P < 0.01$, $^{\&\&\&\&}P < 0.0001$ vs. AP, one-way ANOVA, Tukey's multiple comparison test (*B* and *F*) or two-way ANOVA, Sídák's multiple comparison test (*C*, *D*, and *E*).

endosomes, block endosomal signaling, and provide more efficacious and long-lasting relief from pain than conventional antagonists (9, 11, 15, 17, 22, 40). However, lipidated and nanoparticle-encapsulated drugs are not suited to systemic administration, and pharmacokinetic considerations may limit their usefulness. Thus, the current investigation sought to identify criteria for the rational design of small-molecule antagonists of the NK_1R. The structure of the NK_1R complexed with NT was used to design derivatives of NT (35). NT analogs of variable lipophilicity (LogP, LogD) and acidity (pKa) were synthesized based on the presumption that antagonists with altered physicochemical behavior would penetrate plasma and endosomal membranes and compounds with ideal properties are retained in proximity to NK_1R signalosomes. A similar approach has been used to design fluorinated analogs of fentanyl with a low pKa. These efficiently activate µ-opioid receptors in the acidified extracellular environment of damaged or diseased tissue, and thereby prevent pain without the detrimental on-target side effects usually evoked by engaging µ-opioid receptors in healthy tissues with normal extracellular pH (21, 41). A long residence time of antagonists in endosomes containing the NK_1R might be expected to abrogate endosomal signaling and prevent pain. NT analogs retained the ability to bind to the NK_1R in membrane preparations at extracellular (pH 7.4) and endosomal (pH 6.0) pH, and all potently inhibited SP-induced IP_1 formation. Lipophilic receptor antagonists may better diffuse into endosomes. Moreover, NK_1R conformation may change at a lower pH, conferring a strong and persistent receptor binding of suitable NT analogs. We suggest that PS29 and PS34 show favorable binding properties because such ligands are not charged at the lower pH in endosomes, leading to a more sustained inhibition of endosomal signaling. NT analogs

also potently inhibited SP-induced activation of nuclear ERK, which requires endosomal NK_1R signaling (9). However, whereas AP caused only a transient inhibition of SP-induced activation of nuclear ERK that was rapidly reversed after washout, the inhibition by NT and all NT analogs was maintained after washing cells to remove extracellular drug. Moreover, NT and NT analogs rapidly reversed SP-induced recruitment of $mG\alpha_{sq}$ to endosomes. Notably, the NT analogs PS34 and PS29 caused a considerably larger and more sustained inhibition of capsaicin-evoked allodynia than that of AP and NT, which had smaller and more transient antinociceptive effects. The LogD values of PS29 ($LogD_{5.0}$ = 5.05, $LogD_{7.0}$ = 4.99) and PS34 indicate high lipophilicity. Despite its acidic functional group, the LogD value of PS34 at pH 5 ($LogD_{5.0}$ = 4.90, compared to $LogD_{7.0}$ = 3,49) indicates that deprotonation of PS34 in endosomes is not crucial. Hence, PS34 remains neutral and lipophilic in endosomes. The administration of antagonists by injection into the intrathecal space where they would readily access dorsal horn spinal neurons expressing the NK_1R likely minimizes the possibility that pharmacokinetic differences account for the large and prolonged analgesic actions of PS34 and PS29. Future pharmacokinetic studies are required to fully exclude this possibility. Pharmacokinetic and pharmacodynamic studies are also necessary to determine whether parenterally administered antagonists such as PS34 and PS29 access the NK_1R in endosomes of spinal neurons and effectively alleviate inflammatory and neuropathic pain.

Kinetics and Physicochemical Properties of NK_1R Antagonists. The most basic NT analogs, PS15 and PS49, show the fastest kinetics for the inhibition of endosomal signaling at high concentration. A rapid exchange between the protonated and nonprotonated forms under physiological conditions and pH-dependent protonation states, which are reflected by the experimental LogD values of PS15 ($LogD_{7.0}$ = 5.06, $LogD_{5.0}$ = 3.85), may promote their traffic to endosomes. Additionally, the exchange of the pyridine-core of NT to a more lipophilic benzene-ring (PS analogs) could accelerate the penetration of membranes.

SP-Induced Nociception in Mice Expressing Truncated NK_1R. mRNA encoding NK_1R-311, which lacks most of the intracellular C-terminus, is highly expressed in the human brain (26) and the immune system (42). Lacking critical Ser and Thr residues that are potential sites of GRK phosphorylation and interaction with βARRs, NK_1R-311 is unable to recruit βARRs and does not undergo SP-induced endocytosis (9). The C-terminal domain is also necessary for efficient Gα coupling, since NK_1R-311 responds only to high SP concentrations with reduced and delayed ERK signaling (27, 28). In knockin mice expressing human NK_1R-311, intrathecal injection of SP caused mechanical allodynia, although responses were smaller than those observed in mice expressing human NK_1R-407 or in wild-type mice, which were identical. Although SP caused an initial activation of spinal neurons from NK_1R-311 mice, the sustained response observed in neurons from NK_1R-407 mice was largely absent. Given that the sustained activation of spinal neurons is dependent on NK_1R endocytosis and consequent activation of ERK, the diminished response in neurons from NK_1R-311 mice may be attributable to diminished endocytosis and delayed ERK signaling. However, there are other possible explanations for the diminished nociception in NK_1R-311 mice. The inability of NK_1R-311 to respond to low concentrations of SP and efficiently couple to G proteins may also contribute to diminished nociception. Although altered levels of expression could explain abnormal nociception, the mRNA levels and distribution of the NK_1R were similar in NK_1R-311, NK_1R-407, and wild-type mice. It is also possible that SP may activate receptors other than the NK_1R. SP at high concentrations can activate NK_2R and NK_3R (25), but AP, which is selective for the NK_1R over NK_2R and NK_3R, abolished SP-evoked nociception in NK_1R-311, NK_1R-407, and wild-type mice. It is not possible to exclude the possibility that SP activates other types of GPCRs, such as the mouse Mas–related GPCR MrgprB2, which responds to high concentrations of SP and is antagonized by high concentrations of AP (43). Although MrgprB2 appears to mediate the effects of SP on mouse mast cells, further work is required to determine whether MrgprB2 could be involved in the central actions of SP on nociception in mice.

In summary, lipophilic and acidic NK_1R antagonists cause sustained disruption of endosomal signaling and long-lasting antinociception. The results provide insights into strategies for antagonizing GPCRs in intracellular locations, with implications for designing improved treatments for disease.

Materials and Methods

SI Appendix includes detailed methods.

Design, Synthesis, and Analysis of NT Analogs. The NT-bound NK_1R structure (PDB: 6HLP) (35) was used for molecular docking (44). NT analogs were synthesized by the Suzuki reaction and analyzed by chromatography and mass spectrometry. pKa was determined as described (45). TAMRA-NT binding to membranes from HEK293T cells expressing Nluc-NK_1R was measured using BRET (46). G-protein signaling was assessed by IP_1 assays (47, 48). TAMRA-NT uptake in cells expressing NK_1R-eGFP was studied by confocal microscopy.

BRET. NK_1R trafficking, mGα and βARR2 recruitment, and Gα/Gβγ dissociation were determined by BRET, ebBRET, and nbBRET (16).

FRET. Nuclear ERK activation was measured using nuc-EKAR FRET biosensor (9).

Generation and Characterization of Knockin Mice. Knockin mice were generated expressing full-length (407 aa) or truncated (311 aa) human NK_1R. PCR and RNAScope® probes to human NK_1R-407 and NK_1R-311, specific for human NK_1R-407, or specific for mouse NK_1R, were used to detect NK_1R mRNA. Nociception was studied after intrathecal injection of SP or NK_1R antagonists or intraplanar injection of capsaicin. Mechanical allodynia was assessed by measuring paw withdrawal response to von Frey filaments (9, 17, 49). Cell-attached patch-clamp recordings were made from spinal cord slices (9, 17, 49).

Statistics. Differences were assessed using Student's *t* test for two comparisons and 1- or 2-way ANOVA and Tukey's, Dunnett's, or Šidák's post-hoc test for multiple comparisons. $P < 0.05$ was considered significant at the 95% confidence level.

Data, Materials, and Software Availability. All study data are included in the article and/or *SI Appendix*.

ACKNOWLEDGMENTS. This study was supported by grants from NIH (NS102722, DE026806, DK118971, DE029951, N.W.B. and B.L.S.), Department of Defense (W81XWH1810431, W81XWH2210239, N.W.B. and B.L.S.), National Health and Medical Research Council (NHMRC APP1125877, APP1139586, W.L.I.), and Australian Research Council (ARC DP190102854, W.L.I.). C.J.P. is a Leon Levy Neuroscience Fellow. Cartoons were made with BioRender.

Author affiliations: [a]Department of Molecular Pathobiology, College of Dentistry, New York University, New York, NY 10010; [b]Department of Neuroscience and Physiology, Neuroscience Institute, New York University, New York, NY 10010; [c]Pain Research Center, College of Dentistry, New York University, New York, NY 10010; [d]Department of Chemistry and Pharmacy, Friedrich-Alexander Universität Erlangen-Nürnberg, 91058, Erlangen, Germany; [e]Gene Modification Platform, Monash University, Clayton, VIC 3168, Australia; [f]Drug Discovery Biology, Monash Institute of Pharmaceutical Sciences, Monash University, Parkville, VIC 3052, Australia; [g]NYU Dentistry Translational Research Center, College of Dentistry, New York University, New York, NY 10010; and [h]Department of Physiology and Monash Biomedicine Discovery Institute, Monash University, VIC 3800, Australia

Author contributions: A.H., C.J.P., R.T, P.S., S.T., R.L., H.H., D.W., J.R., N.A.V., D.P.P., D.D.J., B.L.S., W.L.I., P.G., and N.W.B. designed research; A.H., C.J.P., R.T., P.S., S.T., R.L., H.H., D.W., J.R., N.A.V., D.P.P., D.D.J., W.L.I., and P.G. performed research; A.R.B.T. contributed new reagents/analytic tools; A.H., C.J.P., R.T., P.S., S.T., R.L., H.H., D.W., J.R., N.A.V., D.P.P., D.D.J., W.L.I., P.G., and N.W.B. analyzed data; and A.H., C.J.P., R.T., P.S., B.L.S., W.L.I., P.G., and N.W.B. wrote the paper.

1. D. Yang *et al.*, G protein-coupled receptors: Structure- and function-based drug discovery. *Signal Transduct. Target. Ther.* **6**, 7 (2021).
2. V. V. Gurevich, E. V. Gurevich, GPCR signaling regulation: The role of GRKs and arrestins. *Front. Pharmacol.* **10**, 125 (2019).
3. F. Dicker, U. Quitterer, R. Winstel, K. Honold, M. J. Lohse, Phosphorylation-independent inhibition of parathyroid hormone receptor signaling by G protein-coupled receptor kinases. *Proc. Natl. Acad. Sci. U.S.A.* **96**, 5476–5481 (1999).
4. D. Calebiro *et al.*, Persistent cAMP-signals triggered by internalized G-protein-coupled receptors. *PLoS Biol.* **7**, e1000172 (2009).
5. K. A. DeFea *et al.*, The proliferative and antiapoptotic effects of substance P are facilitated by formation of a beta -arrestin-dependent scaffolding complex. *Proc. Natl. Acad. Sci. U.S.A.* **97**, 11086–11091 (2000).
6. K. A. DeFea *et al.*, beta-arrestin-dependent endocytosis of proteinase-activated receptor 2 is required for intracellular targeting of activated ERK1/2. *J. Cell Biol.* **148**, 1267–1281 (2000).
7. A. Godbole, S. Lyga, M. J. Lohse, D. Calebiro, Internalized TSH receptors en route to the TGN induce local Gs-protein signaling and gene transcription. *Nat. Commun.* **8**, 443 (2017).
8. R. Irannejad *et al.*, Conformational biosensors reveal GPCR signalling from endosomes. *Nature* **495**, 534–538 (2013).
9. D. D. Jensen *et al.*, Neurokinin 1 receptor signaling in endosomes mediates sustained nociception and is a viable therapeutic target for prolonged pain relief. *Sci. Transl. Med.* **9**, eaal3447 (2017).
10. N. N. Jimenez-Vargas *et al.*, Endosomal signaling of delta opioid receptors is an endogenous mechanism and therapeutic target for relief from inflammatory pain. *Proc. Natl. Acad. Sci. U.S.A.* **117**, 15281–15292 (2020).
11. N. N. Jimenez-Vargas *et al.*, Protease-activated receptor-2 in endosomes signals persistent pain of irritable bowel syndrome. *Proc. Natl. Acad. Sci. U.S.A.* **115**, E7438–E7447 (2018).
12. A. H. Nguyen, R. J. Lefkowitz, Signaling at the endosome: Cryo-EM structure of a GPCR-G protein-beta-arrestin megacomplex. *FEBS J.* **288**, 2562–2569 (2021).
13. A. H. Nguyen *et al.*, Structure of an endosomal signaling GPCR-G protein-beta-arrestin megacomplex. *Nat. Struct. Mol. Biol.* **26**, 1123–1131 (2019).
14. M. Stoeber *et al.*, A genetically encoded biosensor reveals location bias of opioid drug action. *Neuron* **98**, 963–976.e5 (2018).
15. R. E. Yarwood *et al.*, Endosomal signaling of the receptor for calcitonin gene-related peptide mediates pain transmission. *Proc. Natl. Acad. Sci. U.S.A.* **114**, 12309–12314 (2017).
16. R. Latorre *et al.*, Mice expressing fluorescent PAR2 reveal that endocytosis mediates colonic inflammation and pain. *Proc. Natl. Acad. Sci. U.S.A.* **119**, e2112059119 (2022).
17. P. D. Ramirez-Garcia *et al.*, A pH-responsive nanoparticle targets the neurokinin 1 receptor in endosomes to prevent chronic pain. *Nat. Nanotechnol.* **14**, 1150–1159 (2019).
18. A. R. B. Thomsen, D. D. Jensen, G. A. Hicks, N. W. Bunnett, Therapeutic targeting of endosomal G-protein-coupled receptors. *Trends Pharmacol. Sci.* **39**, 879–891 (2018).
19. J. J. Bowden *et al.*, Direct observation of substance P-induced internalization of neurokinin 1 (NK1) receptors at sites of inflammation. *Proc. Natl. Acad. Sci. U.S.A.* **91**, 8964–8968 (1994).
20. D. Bhansali *et al.*, Nanotechnology for pain management: Current and future therapeutic interventions. *Nano Today* **39**, 101223 (2021).
21. N. N. Jimenez-Vargas *et al.*, Agonist that activates the micro-opioid receptor in acidified microenvironments inhibits colitis pain without side effects. *Gut* **71**, 695–704 (2022).
22. Q. N. Mai *et al.*, A lipid-anchored neurokinin 1 receptor antagonist prolongs pain relief by a three-pronged mechanism of action targeting the receptor at the plasma membrane and in endosomes. *J. Biol. Chem.* **296**, 100345 (2021).
23. P. K. Halik *et al.*, Radiochemical synthesis and evaluation of novel radioconjugates of neurokinin 1 receptor antagonist aprepitant dedicated for NK1R-positive tumors. *Molecules* **25**, 3756 (2020).
24. A. Rizzi *et al.*, In vitro and in vivo pharmacological characterization of the novel NK(1) receptor selective antagonist Netupitant. *Peptides* **37**, 86–97 (2012).
25. M. S. Steinhoff, B. von Mentzer, P. Geppetti, C. Pothoulakis, N. W. Bunnett, Tachykinins and their receptors: Contributions to physiological control and the mechanisms of disease. *Physiol. Rev.* **94**, 265–301 (2014).
26. J. P. Lai, A. Cnaan, H. Zhao, S. D. Douglas, Detection of full-length and truncated neurokinin-1 receptor mRNA expression in human brain regions. *J. Neurosci. Methods* **168**, 127–133 (2008).
27. J. P. Lai *et al.*, Differences in the length of the carboxyl terminus mediate functional properties of neurokinin-1 receptor. *Proc. Natl. Acad. Sci. U.S.A.* **105**, 12605–12610 (2008).
28. S. Spitsin, V. Pappa, S. D. Douglas, Truncation of neurokinin-1 receptor-Negative regulation of substance P signaling. *J. Leukoc. Biol.* 10.1002/JLB.3MIR0817-348R (2018).
29. A. S. Dixon *et al.*, Nanoluc complementation reporter optimized for accurate measurement of protein interactions in cells. *ACS Chem. Biol.* **11**, 400–408 (2016).
30. R. Nehme *et al.*, Mini-G proteins: Novel tools for studying GPCRs in their active conformation. *PLoS One* **12**, e0175642 (2017).
31. Q. Wan *et al.*, Mini G protein probes for active G protein-coupled receptors (GPCRs) in live cells. *J. Biol. Chem.* **293**, 7466–7473 (2018).
32. A. M. van der Bliek *et al.*, Mutations in human dynamin block an intermediate stage in coated vesicle formation. *J. Cell Biol.* **122**, 553–563 (1993).
33. Y. Namkung *et al.*, Monitoring G protein-coupled receptor and beta-arrestin trafficking in live cells using enhanced bystander BRET. *Nat. Commun.* **7**, 12178 (2016).
34. T. Hoffmann *et al.*, Design and synthesis of a novel, achiral class of highly potent and selective, orally active neurokinin-1 receptor antagonists. *Bioorg. Med. Chem. Lett.* **16**, 1362–1365 (2006).
35. J. Schoppe *et al.*, Crystal structures of the human neurokinin 1 receptor in complex with clinically used antagonists. *Nat. Commun.* **10**, 17 (2019).
36. F. Hoffmann-Emery, H. Hilpert, M. Scalone, P. Waldmeier, Efficient synthesis of novel NK1 receptor antagonists: Selective 1,4-addition of grignard reagents to 6-chloronicotinic acid derivatives. *J. Org. Chem.* **71**, 2000–2008 (2006).
37. F. Tuluc, J. P. Lai, L. E. Kilpatrick, D. L. Evans, S. D. Douglas, Neurokinin 1 receptor isoforms and the control of innate immunity. *Trends Immunol.* **30**, 271–276 (2009).
38. G. S. Cottrell *et al.*, Endosomal endothelin-converting enzyme-1: A regulator of beta-arrestin-dependent ERK signaling. *J. Biol. Chem.* **284**, 22411–22425 (2009).
39. D. Roosterman *et al.*, Endothelin-converting enzyme 1 degrades neuropeptides in endosomes to control receptor recycling. *Proc. Natl. Acad. Sci. U.S.A.* **104**, 11838–11843 (2007).
40. R. Latorre *et al.*, Sustained endosomal release of a neurokinin-1 receptor antagonist from nanostars provides long-lasting relief of chronic pain. *Biomaterials* **285**, 121536 (2022).
41. V. Spahn *et al.*, A nontoxic pain killer designed by modeling of pathological receptor conformations. *Science* **355**, 966–969 (2017).
42. J. P. Lai *et al.*, Full-length and truncated neurokinin-1 receptor expression and function during monocyte/macrophage differentiation. *Proc. Natl. Acad. Sci. U.S.A.* **103**, 7771–7776 (2006).
43. E. Azimi *et al.*, Dual action of neurokinin-1 antagonists on Mas-related GPCRs. *JCI Insight* **1**, e89362 (2016).
44. O. Trott, A. J. Olson, AutoDock Vina: Improving the speed and accuracy of docking with a new scoring function, efficient optimization, and multithreading. *J. Comput. Chem.* **31**, 455–461 (2010).
45. X. Liu *et al.*, An allosteric modulator binds to a conformational hub in the beta2 adrenergic receptor. *Nat. Chem. Biol.* **16**, 749–755 (2020).
46. A. Allikalt *et al.*, Fluorescent ligands for dopamine D2/D3 receptors. *Sci. Rep.* **10**, 21842 (2020).
47. J. Hellmann *et al.*, Structure-based development of a subtype-selective orexin 1 receptor antagonist. *Proc. Natl. Acad. Sci. U.S.A.* **117**, 18059–18067 (2020).
48. J. Xu *et al.*, Structural insights into ligand recognition, activation, and signaling of the alpha2A adrenergic receptor. *Sci. Adv.* **8**, eabj5347 (2022).
49. S. R. Chaplan, F. W. Bach, J. W. Pogrel, J. M. Chung, T. L. Yaksh, Quantitative assessment of tactile allodynia in the rat paw. *J. Neurosci. Methods* **53**, 55–63 (1994).